ISSN 1063-7842, Technical Physics, 2011, Vol. 56, No. 12, pp. 1745–1753. © Pleiades Publishing, Ltd., 2011.
Published in Russian in Zhurnal Tekhnicheskoi Fiziki, 2011, Vol. 81, No. 12, pp. 47–55.

GASES AND LIQUIDS

Influence of the Meridional Flow and Thermomagnetic Convection on Characteristics of Magnetic Fluid Seal[1]

M. S. Krakov* and I. V. Nikiforov

Belarussian National Technical University, Minsk, 220013 Belarus
**e-mail: mskrakov@gmail.com*

Received February 24, 2011

Abstract—For the low-speed magnetic fluid seals, the influence of the meridional flow, induced by the shaft rotation, on the distribution of magnetic particles concentration, is studied. Influence of the thermomagnetic convection on the structure of this flow and on the temperature distribution in high-speed magnetic fluid seals is investigated also. The problems were examined by numerical methods. It is discovered that even very slow rotation of the shaft homogenises distribution of the magnetic particles concentration in the seal and thereby enlarges its operation life. For high-speed seals thermomagnetic convection provides the penetration of the fluid flow in the region of the narrow gap and levels off the temperature distribution decreasing its maximum value and thereby enlarges its operation life too. It is found also that the influence of thermomagnetic convection grows with the viscosity increasing.

DOI: 10.1134/S1063784211120103

INTRODUCTION

Magnetic fluid seals (MFS) practically of any design are simplified to the sketch presented on Fig. 1. The rotating shaft, which is made from magnetoconducting material (usually steel), is surrounded by a magnetic system which concentrates the magnetic flux in the narrow gap where the magnetic field strength achieved maximum value (up to $H_{max} \approx 1.5 \times 10^6$ A/m). Situated in this gap the O-ring volume of magnetic fluid plays the role of sealing media.

In static, when shaft rotation is absent, pressure burst Δp for MFS is defined by the expression [1]:

$$\Delta p = \mu_0[(MH)_{max} - (MH)_s], \quad (1)$$

where M is magnetic fluid magnetization, H is strength of magnetic fields, index "max" corresponds to the values in the most narrow part of the MFS gap and index "s"—to the values at the free surface of magnetic fluid.

The magnetic fluid is a colloid solution of magnetic nanoparticles in carrier fluid (average diameter about 10 nm). In the gravity field this solution is stable due to the smallness of particles, sedimentation of the particles in the gravity field is compensated by Brownian motion, and the magnetic fluid remains stable for 10 years. But in the gap of the MFS gradient of the magnetic field so large that effective free fall acceleration is more than acceleration of gravity by 10000 times, i.e., equal to 10000 g. In this situation magnetic particles could not be stabilized by Brownian motion and their concentration in the gap grows. It leads, on the one hand, to the magnetic fluid magnetization growing and, accordingly, to the growing burst pressure in time [2]. On the other hand, this process leads to disintegration of magnetic fluid as a system and could lead to failure of MFS. Shaft rotation could essentially influence the equilibrium concentration distribution of magnetic nanoparticles in the magnetic fluid volume, and these influences depend on the flow pattern in the volume.

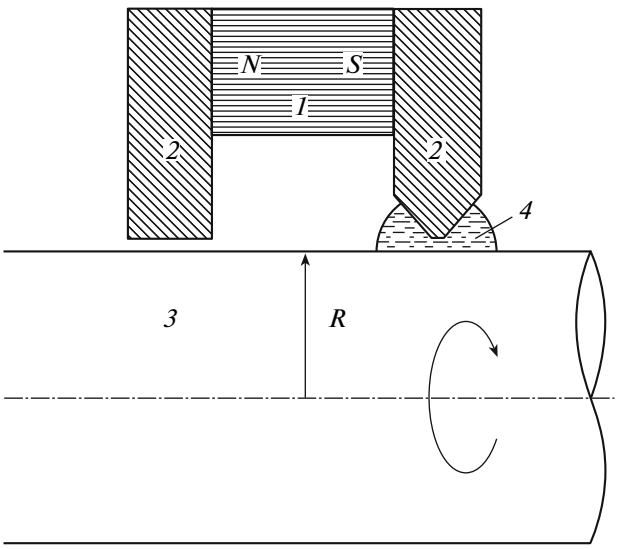

Fig. 1. Scheme of MFS. *1*—permanent magnet, *2*—magnetic circuit, *3*—sealed shaft, and *4*—magnetic fluid.

[1] The article was translated by the authors.

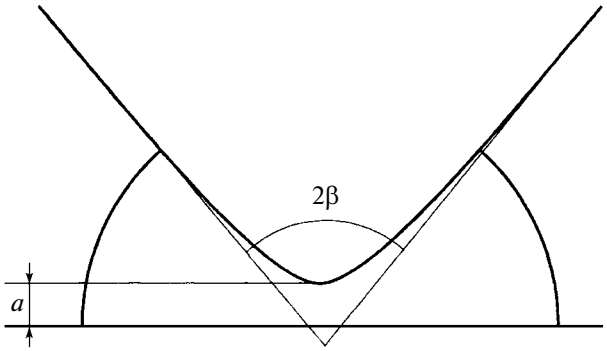

Fig. 2. Problem geometry.

One more aspect of MFS operation which is closely related with the flow in magnetic fluid volume appears at high-speed shaft rotation. As there is heat generation in the magnetic fluid volume due to the viscous friction, the fluid is heated up. Due to the heat removal in the pole of the magnetic system fluid temperature could be stabilized but the character of its distribution in the magnetic fluid volume and maximum value of steady-state temperature will be governed not only by the equations of heat balance but by flow pattern too.

Thus, for analysis of MFS characteristics it is principally important to take into account a meridional flow in the volume of magnetic fluid.

1. GOVERNING EQUATIONS

As the flow in the MFS is axisymmetrical, the well-known Navier–Stokes equation in the cylindrical coordinate system has the form

$$v_r\frac{\partial v_r}{\partial r} + v_z\frac{\partial v_r}{\partial z} - \frac{v_\varphi^2}{r} = -\frac{\partial p}{\partial r} + \nu\left(\frac{\partial^2 v_r}{\partial r^2} + \frac{\partial^2 v_r}{\partial z^2} + \frac{1}{r}\frac{\partial v_r}{\partial r} - \frac{v_r}{r^2}\right), \quad (2)$$

$$v_r\frac{\partial v_\varphi}{\partial r} + v_z\frac{\partial v_\varphi}{\partial z} - \frac{v_r v_\varphi}{r} = \nu\left(\frac{\partial^2 v_\varphi}{\partial r^2} + \frac{\partial^2 v_\varphi}{\partial z^2} + \frac{1}{r}\frac{\partial v_\varphi}{\partial r} - \frac{v_\varphi}{r^2}\right), \quad (3)$$

$$v_r\frac{\partial v_z}{\partial r} + v_z\frac{\partial v_z}{\partial z} = -\frac{\partial p}{\partial z} + \nu\left(\frac{\partial^2 v_z}{\partial r^2} + \frac{\partial^2 v_z}{\partial z^2} + \frac{1}{r}\frac{\partial v_z}{\partial r}\right), \quad (4)$$

and equation of continuity has the form

$$\frac{\partial v_r}{\partial r} + \frac{\partial v_z}{\partial z} + \frac{v_r}{r} = 0. \quad (5)$$

For simulation of the MFS gap we will use the geometrical model proposed in [3]. Within the frame of this model we assume that the pole of the magnetic system, which keeps the magnetic fluid, has the shape of a hyperbole with apex angle 2β, minimal distance between the pole and the shaft surface is a, and the magnetic fluid free surface shape is fixed and coincides with a isoline of the value of magnetic field strength (Fig. 2).

As for a MFS, typical sizes are: for gap width $a \sim 0.2$ mm, for shaft radius $R \sim 20$–50 mm, then, the relation $R \gg a$ is certainly fulfilled. As all derivatives in r and z have an order $1/a$, and the derivative in an angle φ is equal to zero for axisymmetrical flow, and value of r in the Eqs. (2)–(5) has an order R, then this equation system could be essentially simplified. Equations (2), (4), and (5) become

$$v_r\frac{\partial v_r}{\partial r} + v_z\frac{\partial v_r}{\partial z} - \frac{v_\varphi^2}{R} = -\frac{1}{\rho}\frac{\partial p}{\partial r} + \nu\left(\frac{\partial^2 v_r}{\partial r^2} + \frac{\partial^2 v_r}{\partial z^2}\right), \quad (6)$$

$$v_r\frac{\partial v_z}{\partial r} + v_z\frac{\partial v_z}{\partial z} = -\frac{1}{\rho}\frac{\partial p}{\partial z} + \nu\left(\frac{\partial^2 v_z}{\partial r^2} + \frac{\partial^2 v_z}{\partial z^2}\right), \quad (7)$$

$$\frac{\partial v_r}{\partial r} + \frac{\partial v_z}{\partial z} = 0, \quad (8)$$

and for Eq. (3) it is necessary to consider it in more details. Let us use dimensionless velocity and coordinates and choose as a scales linear velocity of the rotating shaft surface V, shaft radius R, and width of the gap a as a representative value for distance when derivatives are calculated. As azimuthal flow v_φ induced by the shaft rotation acts as a source in Eq. (6), then from its left side follows next relationship

$$v_r,\ v_z \sim \sqrt{\frac{a}{R}}\,v_\varphi.$$

Then, Eq. (3) for dimensionless components of velocity could be written in the form

$$\mathrm{Re}\sqrt{\frac{a}{R}}\left(v_r\frac{\partial v_\varphi}{\partial r} + v_z\frac{\partial v_\varphi}{\partial z}\right) = \left(\frac{\partial^2 v_\varphi}{\partial r^2} + \frac{\partial^2 v_\varphi}{\partial z^2}\right), \quad (9)$$

where $\mathrm{Re} = Va/\nu$ is analogous of the Reynolds number. It is supposed below that the relationship $\mathrm{Re}\sqrt{a/R} \ll 1$ is fulfilled and Eq. (9) could be written as

$$\left(\frac{\partial^2 v_\varphi}{\partial r^2} + \frac{\partial^2 v_\varphi}{\partial z^2}\right) = 0. \quad (10)$$

Thus, for further analysis of the magnetic fluid flow in MFS Eqs. (6)–(8) and (10) are used. It is necessary to notice that Eq. (10) gives an opportunity to find the distribution of azimuthal velocity v_φ separately from radial and axial components. The last ones are connected with azimuthal velocity only through the last term in the left side of Eq. (6). So, it is possible to use

the azimuthal velocity found from Eq. (10) for determination of the meridional flow from Eqs. (6)–(8). Due to Eq. (8) it is possible use a stream function ψ so that $v_r = -\partial\psi/\partial z$, $v_z = \partial\psi/\partial r$. Let us use a vortex function $\omega = \mathrm{curl}\mathbf{v}$ for meridional components of velocity and, after differentiation of Eq. (6) in z and Eq. (7) in r, we will receive dimensionless equation for ψ and ω

$$\mathrm{Re}\left(\frac{\partial\psi}{\partial z}\frac{\partial\omega}{\partial r} - \frac{\partial\psi}{\partial r}\frac{\partial\omega}{\partial z}\right) = \frac{\partial^2\omega}{\partial z^2} + \frac{\partial^2\omega}{\partial r^2} + \frac{\mathrm{Re}}{R}\frac{\partial v_\varphi^2}{\partial z}, \quad (11)$$

where the velocity of a shaft surface V, gap width a, and magnetic fluid viscosity ν are used as scales.

2. INFLUENCE OF SHAFT ROTATION ON THE DISTRIBUTION OF THE CONCENTRATION OF MAGNETIC NANOPARTICLES IN MFS AND STABILITY OF MFS CHARACTERISTICS

Under the action of nonuniform magnetic field the magnetic nanoparticles are moving to the area of maximum field, i.e., in the narrowest part of the gap. Concentration of particles would grow in this area infinitely, if not for limiting factors. First of all, it is the diffusion of particles caused by their thermal movement. Under action of the diffusion process particles move in an opposite direction, i.e., from the area with the increased concentration. As the magnetic field is axisymmetrical, transmitting movement of particles lays in the plane r–z. Shaft rotation causes azimuthal movement of the fluid, i.e., directed normal to transmitting movement of particles and, for the first sight, should not influence on their movement in a meridional plane, i.e., on the steady state concentration of particles and, as consequence, on burst pressure of MFS (as the magnetization of the fluid from expression (1), depends on concentration of particles). However, it could be seen from Eq. (11), the solution $\psi = 0$, $\omega = 0$ is possible only in the case

$$\frac{\partial v_\varphi^2}{\partial z} = 0, \quad (12)$$

i.e., the fluid flow could be strictly azimuthal only in an infinite cylindrical gap. If the gap has finite length along a shaft or its border is not parallel to the shaft surface, the condition (12) is not fulfilled and there is a secondary current in the plane r–z. It is obvious, that such current will distribute particles in the volume of a magnetic fluid more homogeneous, i.e., and burst pressure of MFS will change less in time.

For the geometry presented in Fig. 3 it is possible to use coordinates of elliptic cylinder

$$x = c\cos\eta\cosh\xi, \qquad y = c\sin\eta\sinh\xi, \quad (13)$$

where $c = a/\cos\beta$, $0 \le \xi \le \infty$, $0 \le \eta \le 2\pi$. Coordinate x is defined so that $r = R + x$ and directed normal to the MFS shaft surface and coordinate $y = z$ directed along the shaft surface.

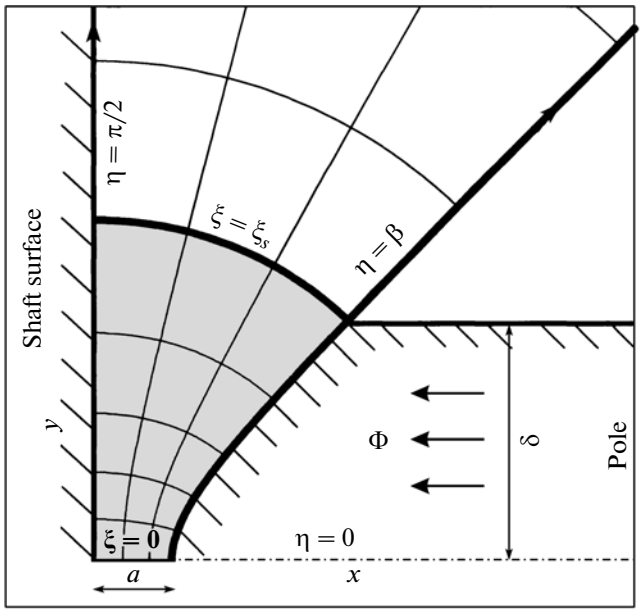

Fig. 3. Calculation domain.

As for steady state distribution of nanoparticle concentration under the pole of the MFS is essentially important magnetic field distribution, we will find the solution of Maxwell's equations in the presented geometry.

We will consider the magnetic permeability of a shaft and an extremely large pole ($\mu = \infty$). As the magnetic field in the gap of the magnetic fluid seal is very high ($H > 10^6$ A/m) and considerably more than a magnetization of magnetic fluid ($M \sim 5 \times 10^4$ A/m), magnetic permeability of a magnetic fluid could be considered equal to permeability of vacuum ($\mu = \mu_0$). It means the magnetic field in a volume of the magnetic fluid is described by the equations

$$\mathrm{div}\mathbf{B} = \mathrm{div}\mu\mathbf{H} = \mu_0\mathrm{div}\mathbf{H} = 0, \quad \mathrm{curl}\mathbf{H} = 0. \quad (14)$$

It is possible to enter function Ψ such that $H_x = \partial\Psi/\partial y$, $H_y = -\partial\Psi/\partial x$. Then, the equation $\mathrm{div}\mathbf{H} = 0$ is satisfied automatically, and the equation $\mathrm{curl}\mathbf{H} = 0$ is reduced to Laplace's equation

$$\Delta\Psi = 0. \quad (15)$$

Solution of Eq. (15) in the coordinate system of the elliptic cylinder has a simple form

$$H = \frac{A}{\sqrt{\sinh^2\xi + \sin^2\eta}}. \quad (16)$$

If the whole magnetic flux Φ induced by a permanent magnet runs through the pole with the thickness 2δ and concentrated in a magnetic fluid volume which is limited by coordinate line ξ_s, than the magnetic field is given by the expression

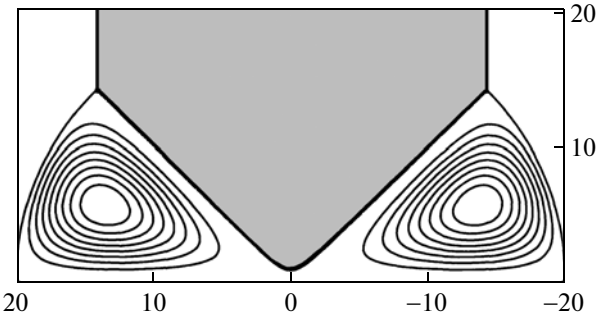

Fig. 4. Typical flow pattern. $\gamma = 10$, $\beta = 45°$, $\mathrm{Re} = 1$, and $\mathrm{R} = 100$.

$$H = \frac{(\Phi/2\delta)\gamma\cos\beta}{\xi_s\sqrt{\sinh^2\xi + \sin^2\eta}}, \tag{17}$$

where $\gamma = \delta/a$.

Equations of motion in the coordinate system (13) become

$$\left(\frac{\partial^2 v_\varphi}{\partial\xi^2} + \frac{\partial^2 v_\varphi}{\partial\eta^2}\right) = 0, \tag{18}$$

$$\omega = -\frac{\cos^2\beta}{(\sinh^2\xi + \sin^2\eta)}\left(\frac{\partial^2\psi}{\partial\xi^2} + \frac{\partial^2\psi}{\partial\eta^2}\right), \tag{19}$$

$$\frac{\partial}{\partial\xi}\left(\frac{\partial\omega}{\partial\xi} - \mathrm{Re}\,\omega\frac{\partial\psi}{\partial\eta}\right) + \frac{\partial}{\partial\eta}\left(\frac{\partial\omega}{\partial\eta} + \mathrm{Re}\,\omega\frac{\partial\psi}{\partial\xi}\right) = \frac{\mathrm{Re}}{R\cos\beta}\left(\cosh\xi\sin\eta\frac{\partial v_\varphi^2}{\partial\xi} + \sinh\xi\cos\eta\frac{\partial v_\varphi^2}{\partial\eta}\right). \tag{20}$$

Once again we will emphasize that the zero solution of Eq. (20) $\omega = 0$, $\psi = 0$ is possible only when $\partial v_\varphi/\partial y = 0$, i.e., only in an infinite gap between cylinders. If the shape of the drop of magnetic fluid differs from cylindrical, then $\omega \neq 0$, $\psi \neq 0$. It means that after shaft rotation besides the azimuthally oriented flow v_φ, the meridional oriented flow v_x, v_y exists in a drop of magnetic fluid. As such a flow lies in the plane of the concentration gradient ($c = c(x, y)$), shaft rotation will influence the distribution of magnetic particles in the volume of magnetic fluid.

The problem of magnetic fluid flow was solved numerically by the finite difference method in the coordinate system of the elliptic cylinder. No-slip conditions were used at solid surfaces: $v_\varphi = 0$ at the surface of a pole, $v_\varphi = 1$ at the shaft surface, $v_x = 0$, $v_y = 0$. Condition of shear stresses equal to zero $\partial v/\partial\eta = 0$ is used at free surface $\xi = \xi_s$ and at the plane of symmetry $\xi = 0$. The typical flow pattern is presented in Fig. 4.

For Brownian particles with concentration c and density ρ the law of mass conservation has a form

$$\rho\frac{\partial c}{\partial t} + \mathrm{div}\mathbf{i} = 0, \tag{21}$$

where $\mathbf{i}$ is the density of mass flux which is equal to

$$\mathbf{i} = -\rho D\nabla c + \rho c b\mathbf{f} + \rho\mathbf{v}. \tag{22}$$

In this expression, D is diffusion coefficient, $b = D/kT$, $\mathbf{v}$ is velocity of fluid flow, and $\mathbf{f}$ is the force acting on the particles by magnetic field. For a spherical particle $b = 1/6\pi\eta R$, where R is a particle radius, η is a dynamic viscosity of fluid, $\mathbf{f} = \mu_0 m\nabla H$, m is a particle magnetic moment, $m = (4/3)\pi R^3 M_I$, and M_I is magnetization of a particle material.

Substitution of expression (22) in Eq. (21) gives an equation for distribution of particle concentration in moving fluid

$$\frac{\partial c}{\partial t} = D\Delta c - \frac{D}{kT}\mu_0 m\nabla H\nabla c - \frac{D}{kT}\mu_0 mc\Delta H - \mathbf{v}\nabla c \tag{23}$$

or in dimensionless form

$$\frac{\partial c}{\partial t} = \Delta c - U\nabla H\nabla c - Uc\Delta H - \mathrm{Re}\,\mathrm{Sc}\,v\nabla c, \tag{24}$$

where $U = \mu_0 m H_0/kT$, $H_0 = \Phi/2\delta$, $\mathrm{Re} = Va/\nu$ is the Reynolds number, $\mathrm{Sc} = \nu/D$ is the Schmidt number, and as the scales the next values are used: a^2/D for time, V (velocity of shaft surface) for fluid velocity, a for distances, and H_0 for magnetic field.

In coordinates of elliptic cylinder, Eq. (24) has the form

$$\frac{\partial c}{\partial t} = \frac{\cos^2\beta}{\sinh^2\xi + \sin^2\eta}\left[\frac{\partial}{\partial\xi}\left(\frac{\partial c}{\partial\xi} - Uc\frac{\partial H}{\partial\xi}\right) + \frac{\partial}{\partial\eta}\left(\frac{\partial c}{\partial\eta} - Uc\frac{\partial H}{\partial\eta}\right) - \mathrm{Re}\,\mathrm{Sc}\left(\frac{\partial c}{\partial\xi}\frac{\partial\psi}{\partial\eta} - \frac{\partial c}{\partial\eta}\frac{\partial\psi}{\partial\xi}\right)\right]. \tag{25}$$

Solution of Eq. (25) was found numerically by the finite difference method. The condition of equality to zero of mass flux at all boundaries of magnetic fluid volume was used as boundary conditions.

As a typical meaning, the next values were used: kinematic viscosity of fluid $\nu = 1.4 \times 10^{-5}$ m^2/s, density $\rho = 1100$ kg/m^3, particles diameter $d = 10^{-8}$ m, and temperature $T = 300$ K. Then, the diffusion coefficient is $D = kT/3\pi\nu\rho d = 2 \times 10^{-12}$ m^2/s and the Schmidt number is equal to $\mathrm{Sc} = 5 \times 10^6$. All variants of simulation were done for the values $\mathrm{Sc} = 5 \times 10^6$, $U = 0.2$; 0.5; 1.0; $\mathrm{Re} = 0$–2.

Modification of the particle concentration profile in magnetic fluid is presented in Fig. 5. It could be seen that the concentration is maximal near the point $\xi = 0$, $\eta = \beta$ (apex of the pole). Also it could be seen that in time particles are distributed in volume more homogeneously.

When concentration of magnetic particles in the volume of the magnetic fluid is not constant, the burst pressure of MFS is not described by Eq. (1) but

defined by pressure difference at the narrowest part of a gap of MFS and at the free surface of magnetic fluid drop

$$\Delta p = p_{\max} - p_s,$$

which must be calculated taking into account variable concentration. Maximum pressure could be found as $p_{\max} = (\mu_0 MH)_{\max} = (\mu_0 M_I cH)_{\max} = \mu_0 M_I (cH)_{\max}$, M_I is magnetization of particles, c is particle concentration from Eq. (21), and H is the strength of the magnetic field from Eq. (17). Accordingly, $p_s = \mu_0 M_I (cH)_s$. It means the burst pressure of the MFS is defined by expression

$$\Delta p = \mu_0 M_I [(cH)_{\max} - (cH)_s]. \quad (26)$$

Maximal and minimal values of isolines cH which cross the volume of magnetic fluid from shaft to pole were found from numerical solutions of Eqs. (17) and (21). Their difference in accordance with (26) was considered as burst pressure of MFS. Figure 6 shows how the value p changes in time for different meanings of parameter U and Reynolds number Re.

Figure 6 shows that for all values of parameter U burst pressure Δp increases in time and achieves some maximal value which is larger as value U increases, i.e., magnetic moment of particles. It means that magnetic fluids with large particles are less stable in MFS. It is necessary to pay special attention to the fact that the maximal value of Δp depends on the Reynolds number: value $(\Delta p)_{\max}$ decreases with increasing of Re. Thus, shaft rotation, which induces secondary meridional flow, agitates the fluid and approximates distribution of particles in the volume of magnetic fluid to homogeneous. Correspondingly, value Δp is approximated to initial value $\Delta p_0 = \mu_0 M_S (H_{\max} - H_s)$, where $c = c_0$.

Figure 7 shows that for Re ~ 2 $\Delta p/\Delta p_0 \approx 1$. It means that in MFS with gap width $a = 2 \times 10^{-4}$ m, fluid viscosity $\nu = 1.4 \times 10^{-5}$ m^2/s even for shaft velocity $V \approx$ 0.1 m/s (i.e., Re ≈ 1.5), and the meridional flow homogenizes particle distribution in the volume of magnetic fluid. As a result, burst pressure of MFS is practically constant in time.

Thus, computer simulation shows that shaft rotation induces secondary circulation flow in the meridional plane which leads to more homogeneous distribution of magnetic particles in the volume of magnetic fluid in MFS. Intensity of the secondary flow is proportional to velocity of shaft rotation. If, in the case on nonmovable shaft, particles concentration in the gap increases in time enlarging finally two–three times, then shaft rotation essentially decreases this enlarging. Even for a shaft rotation about 0.1 m/s nanoparticles concentration in the volume of fluid remains homogeneous and constant in time. It means that even low shaft rotation essentially stabilizes the operating characteristics of MFS.

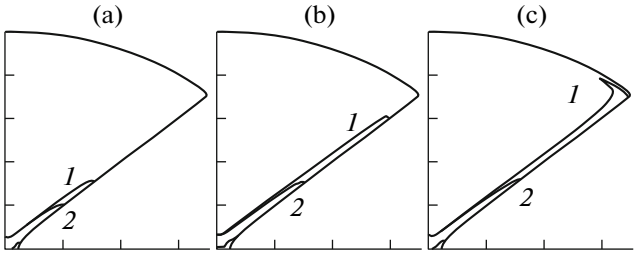

Fig. 5. Isolines of concentration c. t = (a) 1, (b) 3, (c) 5; curve *1*—$c = 1.3$; curve *2*—$c = 1$; Re = 1, $\gamma = 10$, R = 100, and $\beta = 45°$.

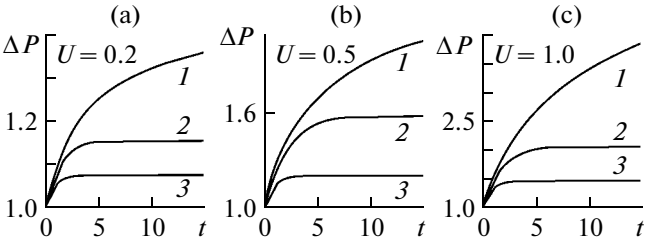

Fig. 6. Dependence of burst pressure of MFS on time. In figures (a, c): Re = (*1*) 0; (*2*) 0.65; and (*3*) 1; (b): Re = (*1*) 0; (*2*) 0.5; and (*3*) 1.

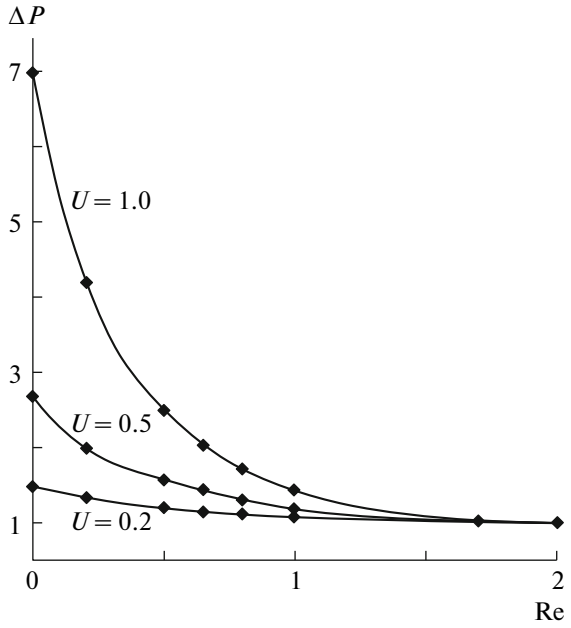

Fig. 7. Dependence of burst pressure of MFS on speed of shaft rotation. $\gamma = 10$, R = 100, and $\beta = 45°$.

3. TEMPERATURE DISTRIBUTION IN WORKING VOLUME OF MFS

Similar to circulatory flow influences on distribution of magnetic particles concentration, it is necessary to expect temperature homogenization in high-speed MFS where magnetic fluid is heated due to viscous friction. This influence was investigated earlier in

[4]. However, in addition to circulatory flow in such kind of MFS one more factor may be essential—natural thermomagnetic convection. At first sight from the usual scales of phenomenon it seems that natural convection is always weaker then induced flow, i.e., it seems improbable that in high-speed MFS where shaft velocity attains 10 m/s natural thermomagnetic convection could be essential for the drop of magnetic fluid with cross-section size no more than 5 mm. However, it is necessary to take into account that magnetic forces in the working volume of MFS are very large. To draw an analogy with gravity forces, then, effective free-fall acceleration in the volume of magnetic fluid attains $g_{\text{eff}} = \mu_0 M\nabla H/\rho \approx (1.28 \times 10^{-6}) \times (4 \times 10^4) \times (10^6/2 \times 10^{-4})/10^3 \approx 10^5$ m/s$^2 \approx 10000\,g$.

Thus, thermomagnetic convection in MFS originated under the influence of the force which is 10000 times more than a gravitational one, so, its intensity could be 10000 times more than intensity of gravitational thermal convection in analogous conditions too. These reasons say that at simulation of a thermal mode of high-speed MFS it is impossible to neglect that natural thermomagnetic convection as differences of temperatures in the volume of a magnetic liquid in such MFS are rather great.

As the vector of magnetic field gradient lies in the meridional plane, components of thermomagnetic buoyancy force are added only in equations for radial and axial components of velocity (6) and (7). In Boussinesq's approximation these equations have the form

$$v_r\frac{\partial v_r}{\partial r} + v_z\frac{\partial v_r}{\partial z} - \frac{v_\varphi^2}{r} = -\frac{1}{\rho}\frac{\partial p}{\partial r} + \nu\left(\frac{\partial^2 v_r}{\partial r^2} + \frac{\partial^2 v_r}{\partial z^2}\right) + \frac{\mu_0}{\rho}\frac{\partial M}{\partial T}(T - T^*)\frac{\partial H}{\partial r}, \quad (27)$$

$$v_r\frac{\partial v_z}{\partial r} + v_z\frac{\partial v_z}{\partial z} = -\frac{1}{\rho}\frac{\partial p}{\partial z} + \nu\left(\frac{\partial^2 v_z}{\partial r^2} + \frac{\partial^2 v_z}{\partial z^2}\right) + \frac{\mu_0}{\rho}\frac{\partial M}{\partial T}(T - T^*)\frac{\partial H}{\partial z}. \quad (28)$$

In the process of standard transition to the variable stream function–vortex these equations become a system of equations

$$\mathrm{Re}\left(\frac{\partial\psi}{\partial z}\frac{\partial\psi}{\partial r} - \frac{\partial\psi}{\partial r}\frac{\partial\psi}{\partial z}\right) = \frac{\partial^2\omega}{\partial z^2} + \frac{\partial^2\omega}{\partial r^2} + \frac{\mathrm{Re}}{R}\frac{\partial v_\varphi^2}{\partial z} - \frac{\mathrm{Gr}_m}{\mathrm{Re}}[\nabla\times(M T\nabla H)]_\varphi, \quad (29)$$

$$\Delta\psi = -\omega,$$

where $\mathrm{Gr}_m = \mu_0\beta_\rho\Delta T_0 H_0 M_S a^2/\rho_0\nu^2$ is the magnetic Grashof number. Here, we assume that $\partial M/\partial T \approx M\beta_\rho$ [1].

The heat transfer equation in the meridional plane has the form (taking into account that $v_r, v_z \ll v_\varphi$):

$$\frac{\partial T}{\partial t} + \mathbf{v}\nabla T = \kappa\Delta T + \frac{\nu}{2c_p}\left[\left(\frac{\partial v_\varphi}{\partial r}\right)^2 + \left(\frac{\partial v_\varphi}{\partial z}\right)^2 - \frac{1}{R}\frac{\partial v_\varphi^2}{\partial r} + \frac{v_\varphi^2}{R^2}\right], \quad (30)$$

where the last term is a heat source due to a viscous friction.

In dimensionless form, Eq. (30) could be rewritten as

$$\mathrm{Pe}\mathbf{V}\nabla T = \Delta T + \mathrm{Pr}\,\mathrm{E}\,\mathrm{Re}^2\left[\left(\frac{\partial v_\varphi}{\partial r} - \frac{v_\varphi}{r}\right)^2 + \left(\frac{\partial v_\varphi}{\partial z}\right)^2\right], \quad (31)$$

where $\mathrm{Pr} = \nu/\kappa$ is the Prandtl number, $\mathrm{Re} = Va/\nu$ is the Reynolds number, $\mathrm{Pe} = \mathrm{RePr}$ is the Pecklet number, $\mathrm{E} = \nu^2/c_p T_0 a^2$, $\mathrm{Gr}_m = \mu_0\beta_\rho\Delta T_0 H_0 M_S a^2/\rho_0\nu^2$, and values $V_0 = 1$ m/s, $\Delta T_0 = 1$ K, and H_0 (maximal value of magnetic field strength under the pole of MFS) are used below as the scales.

As it could be seen from Eq. (27), there are two sources of meridional flow: first, v_φ^2/R is caused by a shaft rotation and is proportional to V^2/R and the reason for the second one is thermomagnetic convection and it is proportional to $\mu_0 M\beta_\rho H_0\Delta T/\rho_0 a$. In the usual situation, the second term is much lower than the first, but in high-speed MFS there is a very high magnetic field gradient together with an extremely large temperature gradient and the situation could be opposite. For example, for $V = 10$ m/s and $R = 5$ cm the first term is about 2×10^3 m/s^2. For typical MFS values of $M_S \sim 4 \times 10^4$ A/m, $H_0 \sim 10^6$ A/m, $\beta_\rho \sim 10^{-3}$ 1/K, $\rho_0 \sim 10^3$ kg/m^3, and $a = 0.2$ mm the second term is about $\Delta T\,(2.5 \times 10^2)$ m/K s^2. It is clear even for temperature differences in the volume of magnetic fluid more than 10 K, the influence of thermomagnetic convection becomes comparable with influence of a shaft rotation. As in high-speed MFS the overheating under the pole could achieve 100 K and more, the importance of taking into account free thermomagnetic convection in this volume is evident.

As is known, the intensity of thermomagnetic convection is proportional to a temperature difference ΔT. The last one is defined by the equation of heat transfer (30) in which the source of heat is viscous friction. So, for temperature difference, it means the intensity of thermomagnetic convection too, is proportional to the viscosity ν. It is a very unusual situation for natural convection which is usually weaker for fluids with high viscosity. As is seen in high-speed MFS the influence of the convection must be more essential for more viscous fluids.

Boundary conditions for the stream function and vortex are found from boundary conditions for veloc-

ity: no-slip conditions at solid borders $\eta = \beta$, $\eta = \pi/2$, condition of symmetry at symmetry plane $\xi = 0$, and condition of zero friction $\partial v/\partial\xi = 0$ at free surface $\xi = \xi_s$.

Boundary conditions for a temperature were chosen from the following considerations. As the steady-state temperature distribution is studied, a heat flux to the rotating shaft after its warming up becomes infinitesimal and could be neglected. So, three boundaries $\eta = \pi/2$ (a shaft), $\xi = 0$ (plane of symmetry), and $\xi = \xi_s$ (free surface) are considered as heat-isolated: $\partial T/\partial n = 0$, where n is a direction normal to the surface.

Also we consider that all dissipative heat is drawn off by a pole cooling system with the cooling fluid with temperature $T_C = 0$. Then, heat transfer condition at the pole surface will have the form

$$-\lambda\frac{\partial T}{\partial n} = \alpha(T - T_C) \text{ or } -\lambda\frac{\partial T}{\partial n} = \alpha T,$$

where vector **n** is directed into the pole and α is a heat transfer coefficient. In dimensionless form this condition could be written as

$$\frac{\partial T}{\partial n} = -\mathrm{Bi}\,T,$$

where $\mathrm{Bi} = \alpha a/\lambda$ is the Biot number. It is well known that the value of the Biot number of about 20 is typical for heat transfer between metal wall and fluid flow. Namely this value was used during numerical simulation.

Equations (29) and (31) were solved numerically by the method of finite difference in the calculation domain presented above (Fig. 3) in coordinates of the elliptic cylinder (13). While constructing a finite-difference scheme a control volume method was used with a linear interpolation function for the stream function and exponential Patankar interpolation function for the temperature and vortex (this function takes into account value and direction of flow velocity in the control volume) [5].

Typical values of the magnetic fluid's physical properties and MFS working volume dimensions were used in the analysis: gap width $a = 2 \times 10^{-4}$ m, apex angle for pole $\beta = 45°$, fluid density $\rho_0 = 1.2 \times 10^3$ kg/m^3, heat conductivity $\lambda = 0.2$ W/(m K), heat capacity $c_p = 1.7 \times 10^3$ J/(kg K), heat diffusivity was equal to $\kappa = \lambda/\rho_0 c_p = 0.2/(1.2 \times 10^3 \times 1.7 \times 10^3) \approx 10^{-7}$ m^2/s, coefficient of thermal expansion $\beta = 10^{-3}$ K^{-1}, and magnetization saturation of magnetic fluid $M_S^* = 4 \times 10^4$ A/m. Shaft surface velocity V (i.e., Reynolds number, Re) was varied during the analysis in such a manner that the overheating was no more than 200 K. The value of the Biot number of 20 was used during the simulation.

The range of viscosities of real magnetic fluids in MFSs is from 3.0×10^{-5} up to 1.5×10^{-3} m^2/s. In this diapason, the Peclet number was ranged from 180000 for minimal viscosity to 13 000 for a maximal one. All calculations were fulfilled using a mesh with 251×151 nodes with test calculations on a refined grid for verification of accuracy of numerical simulation. Since for large Peclet numbers the accuracy of the numerical model was not enough, computations were limited by minimal viscosities equal to 2×10^{-4} m^2/s.

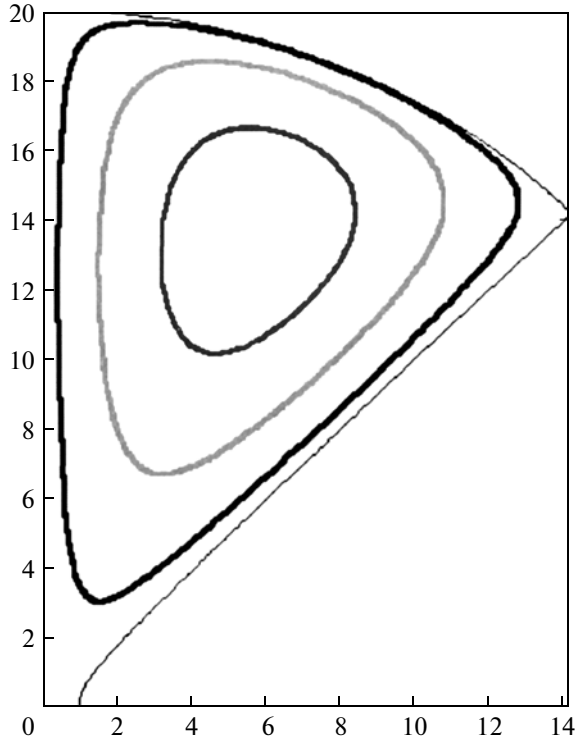

Fig. 8. Stationary flow pattern in meridional plane of MFS. Pr = 5100, E = 3.68×10^{-3}, $\nu = 5 \times 10^{-4}$ m^2/s, Re = 5 (V = 12.5 m/s), and $\mathrm{Gr}_m = 0$.

Figures 8 and 9 represent typical patterns of meridional flow in MFS without free convection ($\mathrm{Gr}_m = 0$) and with free thermomagnetic convection ($\mathrm{Gr}_m = 0.0134$) in the model. These figures show that the flow patterns differ only in the region of the pole apex. The flow modified by thermomagnetic convection (which is especially intensive in the region of high gradients of magnetic field and temperature, i.e., namely in the region of the pole apex, penetrates in the narrowest part of the gap. This means convective heat transfer after this penetration has to be enhanced essentially providing more homogeneous temperature distribution in the volume of magnetic fluid.

Figure 10 shows temperature distribution along the shaft surface for fluid viscosity $\nu = 2 \times 10^{-4}$ m^2/s. Simulation without taking into account (curve *1*) demonstrates that a shaft temperature in the plane of symmetry is very high (194 K more than the temperature of the cooling system). Account of the thermomagnetic convection (curve *2*) lowers essentially maximal temperature under the pole apex (137 K more than the cooling system temperature).

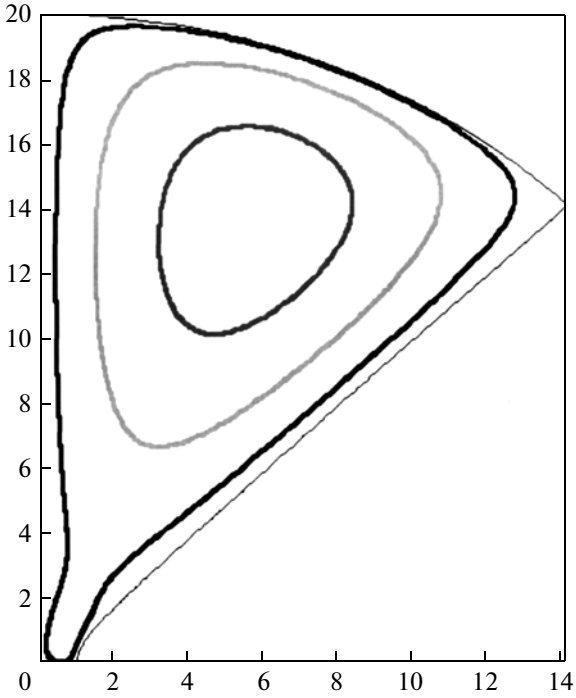

Fig. 9. Stationary flow pattern in meridional plane of MFS. Pr = 5100, E = 3.68×10^{-3}, $\nu = 5 \times 10^{-4}$ m^2/s, Re = 5 (V = 12.5 m/s), and $\mathrm{Gr}_m = 0.0134$.

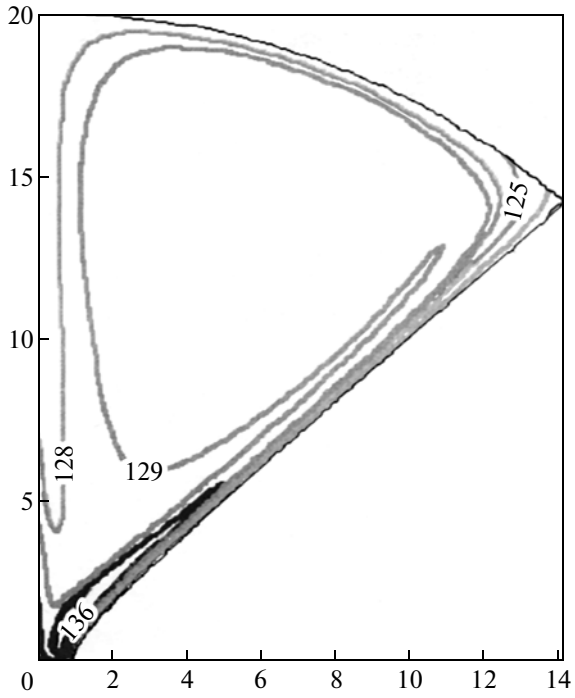

Fig. 11. Temperature distribution in magnetic fluid volume. Pr = 2040, E = 5.88×10^{-4}, $\nu = 2 \times 10^{-4}$ m^2/s, V = 30 m/s, and $\mathrm{Gr}_m = 0.0838$.

More over, Fig. 11 shows that the temperature distribution in the magnetic fluid drop volume is almost uniform due to convective flow.

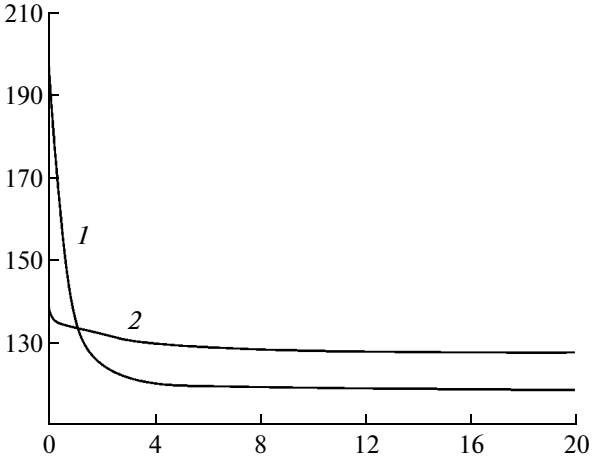

Fig. 10. Dependence of overheating of a shaft (K) on distance from plane of symmetry. Pr = 2040, E = 5.88×10^{-4}, $\nu = 2 \times 10^{-4}$ m^2/s, and V = 30 m/s. Curve *1*—$\mathrm{Gr}_m = 0$, curve *2*—0.0838.

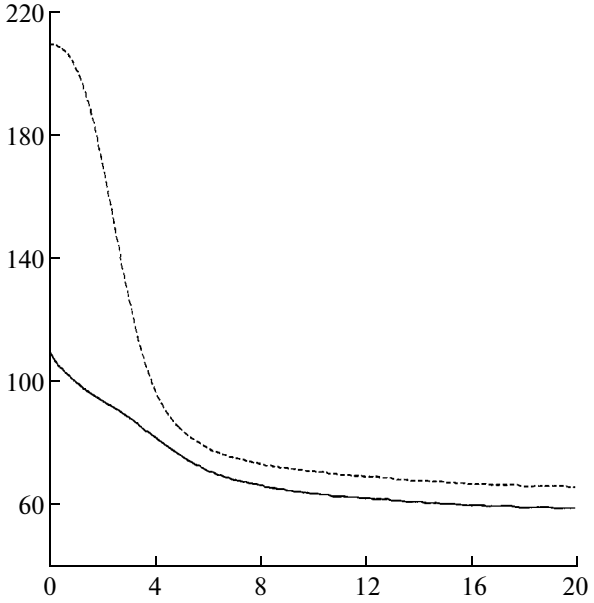

Fig. 12. Dependence of shaft surface temperature on distance from plane of symmetry. Pr = 15300, E = 3.31×10^{-2}, $\nu = 1.5 \times 10^{-3}$ m^2/s, V = 6.38 m/s, dashed line—$\mathrm{Gr}_m = 0$, and solid line—$\mathrm{Gr}_m = 0.00149$.

As is evident from Fig. 12, the influence of thermomagnetic convection on the temperature distribution in high-speed MFS is even more essential for more viscous fluid (for example, the highest temperature of the shaft decreases from 209 to 109 K).

In summary we will notice, that usual intensity of a heatsink due to forced convection increases with growth of fluid flow velocity and, finally sooner or later, becomes more than heatsink due to natural convection which does not depend on outer flow velocity. As in MFS the fluid warming up is determined by viscous dissipation, the overheating of a magnetic fluid grows also with growth of speed of the shaft rotation,

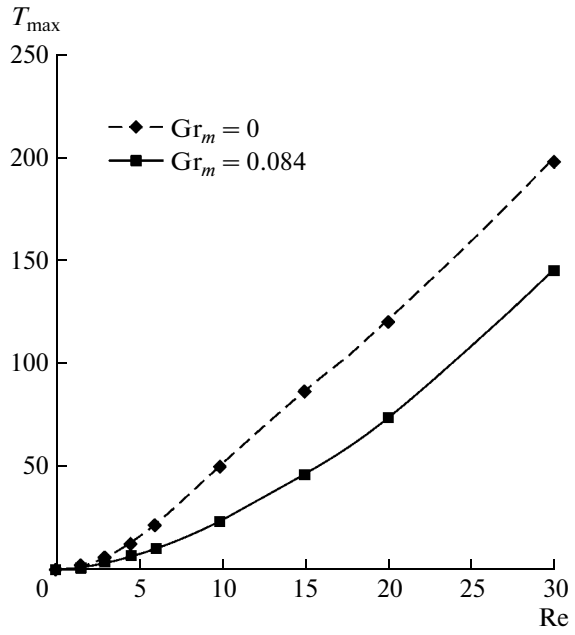

Fig. 13. Dependence of magnetic fluid overheating under the pole apex on a shaft speed rotation. Pr = 2040, E = 5.88×10^{-4}, $\nu = 2 \times 10^{-4}$ m^2/s, and $V_{max} = 30$ m/s.

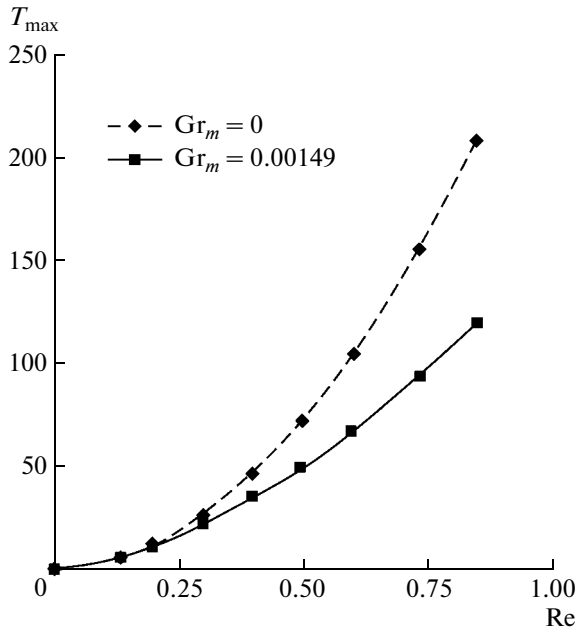

Fig. 14. Dependence of magnetic fluid overheating under the pole apex on a shaft speed rotation. Pr = 15 300, E = 3.31×10^{-2}, $\nu = 1.5 \times 10^{-3}$ m^2/s, and $V = 6.38$ m/s.

i.e., and with growth of meridional flow velocity. This, in turn, leads to an intensification of thermomagnetic convection. Thus, in MFS the situation with thermomagnetic convection becomes twice unique: its influence increases both with growth of viscosity of a magnetic liquid, and with growth of speed of rotation of a shaft. It is shown evidently by the curves presented in Figs. 13, 14.

CONCLUSIONS

Numerical simulation of a meridional flow in the volume of magnetic fluid discovered its the essential influence on characteristics of both static seals and high-speed MFS. In the first case, it is found that even very slow rotation of a shaft leads to homogeneous distribution of magnetic nanoparticles in the volume of magnetic fluid. It means such rotation prevents stratification of magnetic fluid in MFS and thereby essentially increases the operating life of a seal. Also it is discovered in high-speed MFS that it is essential to take into account a thermomagnetic convection which, as became clear, leads to intensive flow directly in the narrowest part of a gap under a pole decreasing the fluid temperature in this area. As is clear from this simulation an operation of MFS is possible for larger speeds as it was considered earlier.

REFERENCES

1. B. M. Berkovskii, V. F. Medvedev, and M. S. Krakov, *Magnetic Fluids* (Khimiya, Moscow, 1989); *Magnetic Fluids: Engineering Applications* (Oxford Science, New York, 1993).
2. S. Taketomi, Jpn. J. Appl. Phys. **19**, 1929 (1980).
3. V. K. Polevikov, Izv. Ross. Akad. Nauk, Mekh. Zhidk. Gaza, No. 3, 170 (1997).
4. B. M. Berkovsky, M. S. Krakov, and S. G. Pogirnitskaya, J. Magn. Magn. Mater. **149**, 101 (1995).
5. S. Patankar, *Numerical Heat Transfer and Fluid Flow* (Hemisphere, 1980).